LA-UR-15-24660
Approved for public release; distribution is unlimited.

Title: Electron-beam dynamics for an advanced flash-radiography accelerator

Author(s): Ekdahl, Carl August Jr.

Intended for: 20th IEEE Pulsed Power Conference, 2015-05-31/2015-06-04 (Austin, Texas, United States)

Issued: 2015-06-22

ELECTRON-BEAM DYNAMICS FOR AN ADVANCED FLASH-RADIOGRAPHY ACCELERATOR *

Carl Ekdahl
Los Alamos National Laboratory, PO Box 1663, Mail Stop P-912
Los Alamos, New Mexico, USA, 87545

Abstract

Beam dynamics issues were assessed for a new linear induction electron accelerator being designed for multi-pulse flash radiography of large, explosively-driven hydrodynamic experiments. Special attention was paid to equilibrium beam transport, possible emittance growth, and beam stability. Especially problematic would be high-frequency beam instabilities that could blur individual radiographic source spots, low-frequency beam motion that could cause pulse-to-pulse spot displacement, and emittance growth that could enlarge the source spots. Beam physics issues were examined through theoretical analysis and computer simulations, including particle-in cell (PIC) codes. Beam instabilities investigated included beam breakup (BBU), image displacement, diocotron, parametric envelope, ion hose, and the resistive wall instability. Beam corkscrew motion and emittance growth from beam mismatch were also studied. It was concluded that a beam with radiographic quality equivalent to the present accelerators at Los Alamos will result if the same engineering standards and construction details are upheld.

I. INTRODUCTION

Flash radiography of explosively driven hydrodynamic experiments is a time proven diagnostic in use world-wide [1,2]. The Advanced Radiography Induction Accelerator (ARIA) is an electron linear induction accelerator (LIA) recently conceived for this purpose [3]. ARIA was proposed to meet the following flash radiography requirements:

- Two or more pulses on a common axis to enable accurate velocity measurements.
- Pulse spacing variable from 200 ns to 3000 ns to accommodate different experiments.
- Each bremsstrahlung radiation pulse less than 50-ns full width at half maximum (FWHM) to minimize motion blur.
- Dose per pulse on axis at 1 m variable from 4 rad to 150 rad for satisfactory signal to noise ratio of radiographs of experiments with vastly different areal densities.
- End-point energy of 3 to 12-MeV to ensure that there is enough useful dose in the energy range of maximum penetrability of the object.
- Spot size less than 0.7-mm FWHM for adequate resolution of details.

The key enabling technology for a reliable multi-pulse LIA is the accelerating cell. For ARIA, the cell design is based on DARHT-I, but with the ferrite cores replaced with Metglas to provide enough flux swing (volt-seconds) for four pulse operation.

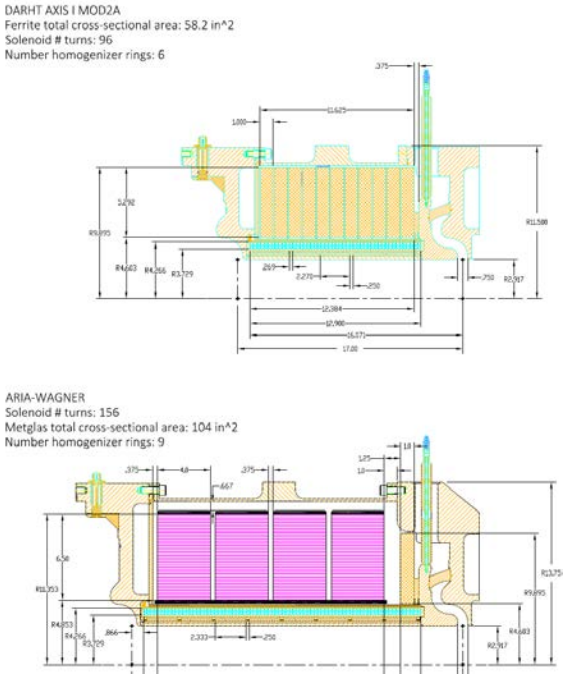

Figure 1. Comparison of ferrite loaded DARHT-I cell (top) and Metglas loaded ARIA cell (bottom). Note that gap and cavity of ARIA is identical to DARHT-I, including first ferrite disk.

The cells are designed to operate at 250 kV with a 2-kA beam load. The accelerating gap, cavity shape, and cavity wall materials of the cell are identical to the DAHRT-I

* Work supported by the National Nuclear Security Administration of the U. S. Department of Energy under contract number DE-AC52-06NA25396

cell in order to have the same BBU properties (see Fig. 1). Each cell incorporates a solenoid and steering dipoles as on DARHT-I.

Except for cell dimensions, the physical layout of the accelerator is the same as DARHT-I, with cells grouped in blocks of four, and pumping stations between blocks of eight. There are external Helmholtz coils located to provide magnetic guide field in the gaps between blocks of eight. Between 36 and 44 cells are required to reach the 12-MeV maximum energy, if the injected energy is in the range of designs being considered (1.5 MeV to 3.0 MeV).

The high-quality DARHT-I electron beam produces bremsstrahlung radiation source spots exceeding all anticipated requirements for hydrodynamic testing. However, there are enough differences between ARIA and DARHT-I that an assessment of beam dynamic issues in ARIA is called for. These issues include beam transport, motion, stability, and emittance. Effective management of these issues has consequences for accelerator engineering choices. An initial investigation of these issues based on a preliminary design for ARIA is the purpose of this article.

To assess the beam dynamics issues on ARIA, we relied on analytic theory, simulation codes, and experimental data from the DARHT LIAs.

II. BEAM TRANSPORT

The electron beam is transported through the ARIA LIA using solenoidal magnetic focusing fields. This is an efficient and convenient means that has been used in all electron LIAs since the very first. Each accelerating cell has a solenoid incorporated into it, as well as dipole windings for steering. The magnetic field produced by these magnets is called the tune of the accelerator. This section reports the results of beam simulations of tunes for ARIA. The most accelerator cells (44) are required by the lowest injector energy (1.5 MeV), and that is the configuration reported here, since it is the most susceptible to beam instability. The initial 2-kA, 1.5-MeV beam produced by the injector was assumed to have a normalized emittance $\varepsilon_n = 300\,\pi$-mm-mr, and an envelope radius of 5 cm at an anode focusing solenoid located 97 cm upstream of the first cell solenoid.

We use the XTR envelope code [4] for designing tunes for DARHT. This code was also used to develop tunes for the ARIA accelerator design. A tune for the 44-cell ARIA that is comparable to the nominal DARHT-I tune is shown in Fig. 2.

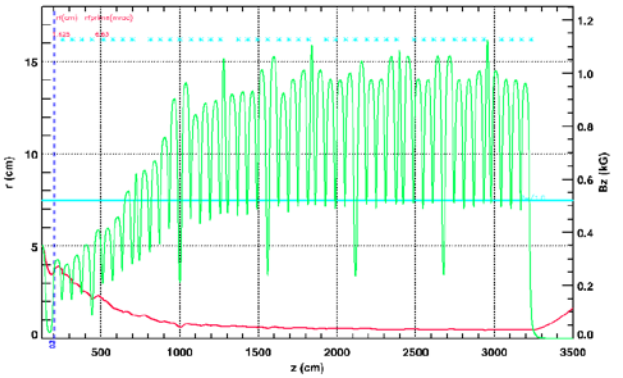

Figure 2. Nominal tune for ARIA with a 1.5-MeV injected beam. (red) Beam envelope, left scale. (green) Magnetic guide field on axis, right scale. (solid cyan) Beam pipe wall. (cyan asterisks) Accelerating cell potential.

Emittance growth can result from envelope oscillations caused by a mismatch of the beam to the magnetic transport system. Beam emittance growth in the ARIA LIA was assessed using a particle-in-cell (PIC) code based on the Large Scale Plasma (LSP) code [5]. The on-axis magnetic field (B_z) for the PIC simulations was extracted from the XTR simulations, and the on-axis electric accelerating field (E_z) was obtained from an electrostatic simulation of the gaps.

Using the XTR initial conditions for the PIC simulations the ARIA tune produced no emittance growth (Fig. 3), even though the PIC results showed mild envelope oscillations not evident in the XTR envelope calculations. However, these oscillations are insufficient to cause emittance growth.

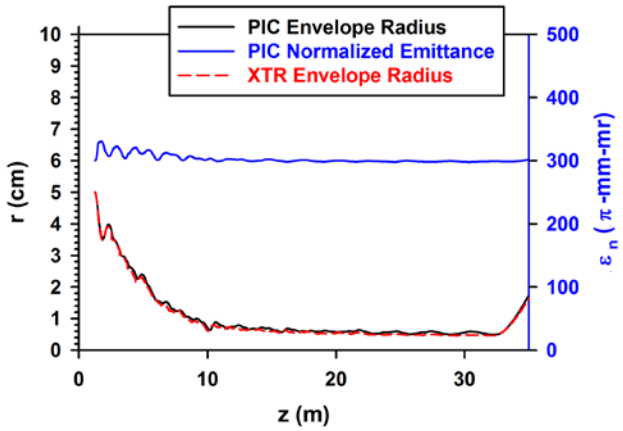

Figure 3. PIC simulation of ARIA tune. Black curve: ARIA beam envelope calculated by PIC code. Blue curve: Beam emittance calculated by PIC code. Also shown for comparison is the envelope calculated by XTR (Red dashed curve).

To test the robustness of the tune to mismatched beam initial conditions, the PIC code was run using the same initial conditions, but into a higher magnetic focusing field. Figure 4 shows the results of PIC simulations with

the magnetic field increased by 5 %. The envelope oscillations induced by this mismatch are sufficient to cause 30% - 50% growth of the beam emittance. The detailed mechanism of this contribution to emittance growth is parametric amplification of electron orbits that resonate with the envelope oscillation, expelling those electrons from the beam core into a halo [6, 7, 8].

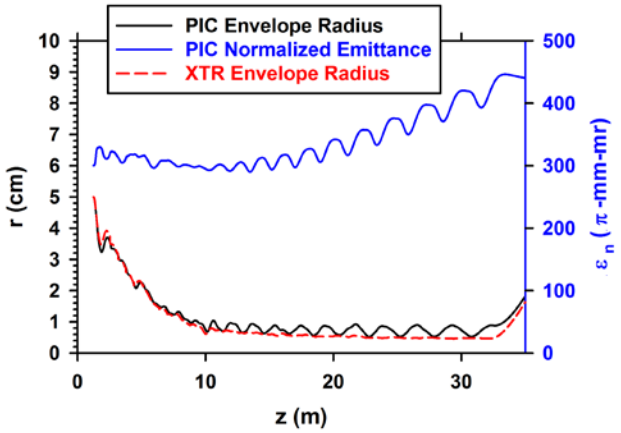

Figure 4. PIC simulation of ARIA with solenoidal focusing field increased by 5%. Black curve: ARIA beam envelope calculated by PIC code showing oscillations produced by mismatch of the beam to the tune. Blue curve: Beam emittance calculated by PIC code showing growth caused by these envelope oscillations. Also shown for comparison is the matched envelope calculated by XTR (Red dashed curve).

III. BEAM STABILITY

A. *Beam Breakup*

The most dangerous instability for electron linacs is the beam breakup (BBU) instability [9, 10]. For radiography LIAs it is particularly troublesome, because even if it is not strong enough to destroy the beam, the high-frequency BBU motion can blur the source spot , which is time-integrated over the over the pulselength. In a fast risetime LIA such as DARHT-I or ARIA, BBU excited by the sharp beam head grows to a peak and then decays [9] (unlike on the slowly rising beam of DARHT-II, where BBU grows from noise and corkscrew throughout the pulse [10]). For a large enough number of accelerating cells, theory predicts that the BBU growth asymptotes to

$$\xi(z) = \xi_0 \left[\gamma_0 / \gamma(z)\right]^{1/2} \exp\left(\Gamma_m\right) \qquad (1)$$

where subscript zero denotes initial conditions, and γ is the relativistic mass factor. The exponent in this equation is

$$\Gamma_m(z) = \frac{I_{kA} N_g Z_{\perp\Omega/m}}{3\times 10^4} \left\langle \frac{1}{B_{kG}} \right\rangle \qquad (2)$$

where I is the beam current (kA), N_g is the number of accelerating gaps, $Z_\perp$ is the transverse impedance (Ω/m), B is the guide field (kG), and $\langle\ \rangle$ indicates an average over z [10]. This theoretical maximum amplitude of the BBU in high-current LIAs has been experimentally confirmed [12, 13], was implemented in our XTR envelope code, and used to design DARHT-II tunes that suppress BBU amplification to acceptable levels [14,15] .

`For ARIA, we will use the exact gap and cavity geometry as DARHT-I to make the transverse impedance the same, thereby ensuring that BBU will be suppressed as well as in DARHT-I. The transverse impedance is proportional to the quality factor, Q, of the cell, which is fundamentally the electromagnetic energy stored divided by the energy dissipated by Ohmic heating of the walls. Therefore, if the geometry and wall materials of the ARIA cells are exactly the same as those of the DARHT-1cells, one can also expect the transverse impedance to be exactly the same. Thus, for the same currents, one can compare the relative stability of different geometries and tunes by simply comparing $N\langle 1/B\rangle$.

Using the asymptotic scaling formula (Eq. (2)) to compare the BBU characteristics of DARHT-I with ARIA tuned as in Fig. 1 it is found that ARIA would be more stable using either a high-or low energy injector, and the required number of cells to achieve 12 MeV (Table I).

Table I. BBU properties of tunes

	KE_0 MeV	N_{cells}	$\langle 1/B\rangle$ kG^{-1}	$N_{cells}\langle 1/B\rangle$ kG^{-1}
DARHT-I	3.8	64	1.27	81.3
ARIA	3.0	36	1.88	67.7
ARIA	1.5	44	1.41	62.0

B. *Corkscrew Motion*

Strictly speaking, corkscrew motion [16] (or beam sweep [14]) is not an instability. Rather, it is the result of temporal variation of the beam energy interacting with transverse magnet fields in the LIA. The beam deflection by these fields is roughly inversely proportional to beam energy, so time varying beam energy causes time varying deflections that manifest themselves as corkscrew or sweep at the accelerator exit. High-frequency corkscrew during the pulse flat top is particularly worrisome, because it can seed the BBU.

The amplitude of the corkscrew is approximately [17]

$$A \approx \sqrt{N}\,\delta\ell\,\frac{\delta\gamma}{\gamma}\phi_{total} \qquad (3)$$

where $A^2 = \langle \delta x^2 \rangle_t + \langle \delta y^2 \rangle_t$ over a time t ; $\delta x = x - \langle x \rangle$. Also, N is the number of magnets, $\delta\ell$ is the rms misalignment, and ϕ_{total} is the total phase advance ($\int k_\beta\, dz$). The cell misalignment includes both offset and tilt, with the tilt contribution approximately the solenoid

length times the rms tilt angle (in quadrature with the rms offset). Measured misalignments on DARHT-II were 0.3-mr rms tilt and 0.1-mm rms offset of the 38-cm long solenoids, giving $\delta\ell$ <0.2 mm. The pulse flattop energy variation on DARHT-I is $\delta\gamma/\gamma$ < 0.1%. We use these values for ARIA, since we will apply DARHT-like engineering standards. A comparison of corkscrew between LIAs is shown in Table II.

Table II: Corkscrew properties of tunes

	KE_0 MeV	N_{cells}	ϕ	$N^{1/2}\phi$
DARHT-I	3.8	64	25.9	207
ARIA	3.0	36	22.8	137
ARIA	1.5	44	43.7	290

Even though the 44-cell ARIA appears to be slightly worse than DARHT-I, the corkscrew amplitude would be less than 1 mm. Furthermore, significant reduction of corkscrew can be achieved by application of corrector dipoles in the cells [18] as was done on DARHT-II [8].

Operationally, the most straightforward means for reducing the BBU is to increase the magnetic guide field. However, this also increases the corkscrew. On the other hand, it is clear from Eq. (1), Eq. (2), and Eq. (3) that corkscrew only depends linearly on *B*, whereas BBU is suppressed exponentially. This is illustrated in Fig. 5, where it is seen that BBU is reduced by more than a factor of 5 with only a 50% increase in corkscrew. Moreover, a modest 20% increase in the field would reduce BBU by a factor of ~2.5, and minimize the motion by equalizing the contribution from BBU and corkscrew. Thus, increasing the magnetic field to suppress BBU is an effective strategy.

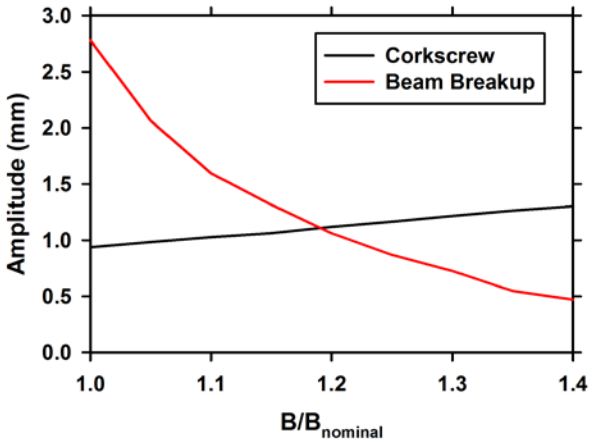

Figure 5. Amplitude of BBU and corkscrew as functions of solenoidal focusing field strength for typical ARIA parameters.

C. Image Displacement Instability

The image displacement instability (IDI) is also the result of a slightly offset beam interacting with a cavity [19, 20, 21]. Whereas the BBU is the result of specific cavity resonances interacting with the beam, the IDI has no frequency dependence, because it is the result of the difference of magnetic and electric field boundary conditions, so it can perturb the beam even at the lowest frequencies. Moreover, unlike the BBU, the IDI has a definite stability threshold. That is, the beam is unstable in a guide field less than $B_{\min}(\gamma, I_b)$, which a function of beam energy, current, and accelerator geometry.

In a beam pipe a slightly offset beam is attracted to the wall by the image of its space charge, and repelled from the wall by the image of its current. These forces balance to within $1/\gamma^2$, with the net force being attractive toward the wall. This is normally counterbalanced by the focusing field. However, in the vicinity of a gap in the wall, the induced charge on the wall collects at the gap edges, and the electric field of the beam decays with radius much more rapidly in the cavity than in the pipe. Thus, if the gap is short compared to the tube radius, the position of the image line charge is almost unchanged. On the other hand, the azimuthal magnetic field of the beam decays with radius exactly as in a pipe with radius equal to the outer wall of the cavity, and the effect is as if the current image was located at a greater distance, reducing the repulsive force from the wall. If the focusing field is too weak, the beam will be displaced toward the wall, and this effect will cumulate as the beam transits each successive gap.

Two recent approaches to IDI theory treat the problem in the limit of a narrow gap for a deep cavity, and neglect the magnetic repulsive force in the vicinity of the gap [21, 22]. Bothe find stability for $B > B_{\min} \propto (I\gamma)^{1/2}$ with differing constants of proportionality, but both theories predict stability for the magnetic fields of ARIA.

D. Diocotron Instability

The ARIA diode design used for this investigation incorporated measures to prevent the creation of a hollow beam profile, because hollow beams in axial magnetic fields can be diocotron unstable [23, 24, 25]. The theory of this instability is well founded and has been validated by numerous experiments with relativistic electron beams. Under some conditions, it may be evident on the DARHT-I beam when it is tightly focused by the anode magnet. It would be a troublesome source of beam emittance if it were present on the ARIA beam.

The diocotron is an interchange type of instability caused by sheared rotational velocity in a beam with a radial density profile having an off-axis maximum, as in a hollow beam with cupped "inverted" profile [24]. In a uniform axial magnetic field, the rotational shear is due to the $\mathbf{E}\times\mathbf{B}$ drift produced by beam space charge, which alters the rigid rotation already present from conservation of canonical angular momentum.

The instability is characterized by strength parameter

$$s = q = \omega_p^2 / \omega_c^2 \qquad (4)$$

where $\omega_p^2 = e^2 n_e / \gamma m_e \varepsilon_0$ and $\omega_c = eB / \gamma m_e$. Thus, $s = \gamma n_e m_e / \varepsilon_0 B^2$. Numerical and experimental investigations have shown that high current, hollow beams can be unstable for s < 0.1, depending on the gradient of the current profile, with sharper gradients being the most (5)unstable. Moreover, theory predicts that the growth rate of the instability is proportional to ω_D / γ^2, where $\omega_D \equiv \omega_p^2 / 2\omega_c = en_e / 2\varepsilon_0 B$ is the diocotron frequency. Thus, low energy beams are the most susceptible to this instability, and have the fastest growth rates.

The peak of the anode magnet field at the ARIA diode exit is B ~ 350 G, and the envelope radius is ~ 5 cm. For the 1.5-MeV, 2-kA ARIA beam exiting the diode, s ~ 1.8, so it should be stable. However, reduction of the current, or increasing the anode magnet strength significantly should be approached with caution, especially if the diode produces a hollowish beam.

E. Resistive Wall Instability

The resistive wall instability is a problem for long-pulse LIAs, but should not be an issue for ARIA. The instability is caused by the beam magnetic field diffusion into the beam-tube wall, whereas the induced charge remains on the surface [26]. Thus, just as for the IDI, the beam is more strongly attracted to the wall. This attraction grows in time as the characteristic magnetic penetration time, so a long pulse beam exhibits a growing head-to-tail displacement. The instability is characterized by a length over which it shows significant growth;

$$\Lambda = 5.6 \frac{B_{kG} b_{cm}^3}{I_{kA} \sqrt{\rho_{\mu\Omega-cm} \tau_{\mu s}}} \text{ meters} \qquad (5)$$

For ARIA parameters in a stainless steel beam pipe the characteristic length is $\Lambda = 587 B_{kG}$ m, and for fields greater than the minima required to defeat the IDI (> 0.23 kG), the characteristic length for growth is much longer than the ARIA LIA, so it should notbe a problem.

F. Ion Hose Instability

Another instability that can be dangerous for a long pulse accelerator is the ion-hose instability [27]. This is caused by beam-electron ionization of residual background gas. The space-charge of the high-energy beam ejects low-energy electrons from the ionized channel, leaving a positive channel that attracts the beam electrons back if they wander away. This causes the beam to oscillate about the channel position. Likewise, the electron beam attracts the ions, causing them to oscillate about the beam position. Because of the vast differences in particle mass the electron and ion oscillations are out of phase, and the oscillation amplitudes grow.

This instability was of some concern for the long-pulse DARHT Axis-II LIA, and a substantial effort was devoted to understanding it through theory and experiments. The theory of the ion-hose instability in a strong axial guide field such in DARHT-II has been developed in analogy to BBU by treating the forces as a transverse impedance [28], and more recently through the use of a spread-mass model [29]. The predictions of these analytic models are in agreement with PIC code simulations [29], including the saturation in time to a maximum growth exponent Γ_m in analogy to the BBU. From the theory and PIC simulations the maximum growth exponent for ion hose is

$$\Gamma_m = 0.043 I_{kA} \tau_{\mu s} L_m \left\langle p_{\mu Torr} / \left(B_{kG} a_{cm}^2 \right) \right\rangle \qquad (6)$$

where the brackets denote averaging over the LIA length L. We experimentally confirmed this on DARHT Axis-II over a wide range of beam parameters in different gasses over a wide range of ion mass [1].

Setting $\Gamma_m \le 0.693$ for ARIA will ensure that the vacuum is low enough to inhibit the growth of this instability. Using XTR to calculate $\left\langle 1/\left(Ba^2 \right) \right\rangle$ gives the required background pressure for stability; p<1.5E-6 Torr. This requirement is easily met, since DARHT-I operates at p<1.0E-7Torr.

G. Parametric Envelope Instability

As seen in Fig. 2, the ARIA magnetic focusing field is periodically modulated. Therefore, the focusing forces on the beam are also periodically modulated. Moreover, the envelope of a slightly mismatched beam undergoes m=0, "breathing mode" oscillations (see Fig. 4, for example). Under some circumstances, beam transport in a spatially modulated magnetic field can cause a parametric instability of beam envelope oscillations, which in turn could cause halo and emittance growth [6]. This is most problematic for low energy coasting beams, so would only be an issue for ARIA if it is operated in a mode for low-dose radiography like presently done with Cygnus. Figure 6 shows an envelope code simulation of this instability on a low-energy coasting beam.

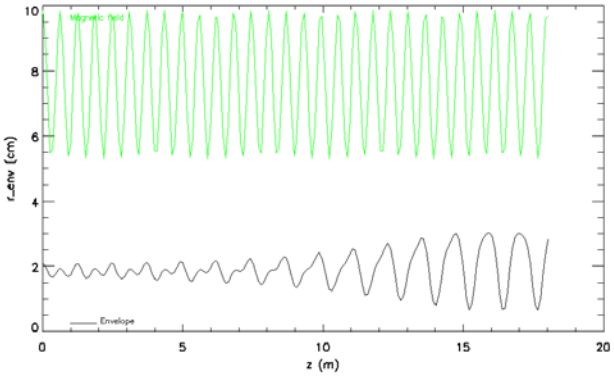

Figure 6. Unstable envelope oscillations of a low-energy beam coasting in a periodic guide field. (black) Beam envelope. (green) Solenoidal focusing field.

An analytic theory of this instability [30] reduces the envelope equation to the well-known Mathieu equation that describes oscillatory physical systems with periodically varying parameters, the solutions of which have distinct regions of instability. For ARIA beam parameters, these regions are very small, so it is unlikely that a low-dose tune would cause instability. Moreover, beam acceleration/deceleration in this mode tends to stabilize. On the other hand, this issue must be carefully examined if ARIA is to be operated in a low-dose mode.

IV. SUMMARY

In general, if the engineering standards used on the DARHT accelerators are adhered to, there should be minimal issues with beam dynamics on ARIA. Of course, commissioning such a machine will involve developing and testing magnetic tunes, including the use of corrector dipoles in some of the cells. However, based on these simulations and calculations, we do not expect disruptive instabilities or excessive emittance growth in ARIA.

V. REFERENCES

[1] C. Ekdahl, "Modern electron acccelerators for radiography," IEEE Trans. Plasma Sci., vol. 30, no. 1, pp. 254-261, 2002.

[2] K. Peach and C. Ekdahl, "Particle radiography," Rev. Acc. Sci. Tech., 2013.

[3] M. Crawford, "ARIA Advanced radiography induction accelerator," Los Alamos National Laboratory report LA-UR-14-20805, 2014.

[4] P. Allison, "Beam dynamics equations for XTR," Los Alamos National Laboratory report, LA-UR-01-6585, 2001.

[5] C. Thoma and T. P. Hughes, "A beam-slice algorithm for transport of the DARHT-2 accelerator," in *Part. Acc. Conf.*, 2007.

[6] R. L. Guckstern, “Analytic model for halo formation in high current ion linacs,” Phys. Rev. Lett., vol. 73, (1994), p. 1247.

[7] T. P. Wangler, et al., “Particle-core model for transverse dynamics of beam halo,” Phys. Rev. Special Topics- Accel. Beams, vol. 1, (1998), p. 084201.

[8] C. Ekdahl, "Tuning the DARHT long-pulse linear induction accelerator," IEEE Trans. Plasma Sci., vol. 41, pp. 2774 - 2780, 2013.

[9] W. K. H. Panofsky and M. Bander, "Asymptotic theory of beam-breakup in linear accelerators," Rev. Sci. Instrum., vol. 39, pp. 206-212, 1968.

[10] V. K. Neil, L. S. Hall and R. K. Cooper, "Further theoretical studies of the beam breakup instability," Part. Acc., vol. 9, pp. 213-222, 1979.

[11] Y. Y. Lau, "Classification of beam breakup instabilities in linear accelerators," Phys. Rev. Lett., vol. 63, pp. 1141 - 1144, 1989.

[12] C. Ekdahl and et al., "Long-pulse beam stability experiments on the DARHT-II linear induction accelerator," IEEE Trans. Plasma Sci., vol. 34, pp. 460-466, 2006.

[13] J. Coleman and et al., "Increasing the intensity of an induction accelerator and reduction of the beam breakup instability," Phys. Rev. ST Accel. Beams, vol. 17, pp. 030101, 1 -11, 2014.

[14] C. Ekdahl and et al., "Beam dynamics in a long-pulse linear induction accelerator," J. Korean Phys. Soc., vol. 59, pp. 3448 - 3452, 2011.

[15] C. Ekdahl and et al., "Suppressing beam motion in a long-pulse linear induction accelerator," Phys. Rev. ST Accel. Beams, vol. 14, p. 120401, 2011.

[16] Y.-J. Chen, "Corkscrew modes in linear induction accelerators," Nucl. Instrum. Methods Phys. Res., vol. A292, pp. 455 - 464, 1990.

[17] Y.-J. Chen, "Transverse beam instabilityin a compact dielectric wall induction accelerator," in Part. Acc. Conf., Knoxville, TN, 2005.

[18] Y.-J. Chen, "Control of transverse motion caused by chromatic aberration and misalignments in linear accelerators," Nucl. Instrum. Methods Phys. Res., vol. A398, pp. 139 - 146, 1997.

[19] C. H. Woods, "The image instability in high current accelerators," *Rev. Sci. Instrum.*, vol. 41, pp. 959 - 962, 1970.

[20] R. Adler and et al., "The image-displacement effect in intense electron beams," Part. Acc., vol. 13, pp. 25 - 44, 1983.

[21] R. Briggs, "Personal communication," 2005.

[22] G. J. Caporaso and Y.-J. Chen, "Electron Induction Linacs," in Induction Accelerators, K. Takayama, Ed., Bearlin, DE, Springer-Verlag, 2011, pp. 117 - 163.

[23] R. H. Levy, "Diocotron instability in a cylindrical geometry," Phys. Fluids, vol. 8, pp. 1288 - 1295, 1965.

[24] R. C. Davidson and G. M. Felice, "Influence of profile shape on the diocotron instability in a non-neutral plasma column," Phys. Plasmas, vol. 5, pp. 3497 - 3511, 1998.

[25] R. B. Miller, An introduction to the physics of intense charged particle beams, New York, NY: Plenum Press, 1982, pp. 126, et seq..

[26] G. Caporaso, W. Barletta and V. K. Neil, "Transverse resistive wall instability of a relativistic electron beam," *Part. Accel.*, vol. 11, pp. 71 - 79, 1980. H. L. Buchanan,

[27] "Electron beam propagation inthe ion-focussed regime," Phys. Fluids, vol. 30, pp. 221 - 231, 1987.

[28] R. Briggs, "Transverse instabilities from ion oscillations in the DARHT-II accelerator," Lawence Berkeley National Laboratory report, M7848, 2000.

[29] T. Genoni and T. Hughes, "Ion-hose instability in a long-pulse linear induction accelerator," Phys. Rev. ST-Accel. Beams, vol. 6, p. 030401, 2003.

[30] C. Ekdahl, “Beam dynamics for ARIA,” Los Alamos National Laboratory Report LA-UR-27454, 2014 and arXiv:1503.06824[physics.acc-ph]